

On Modelling the Roles Played by Diffusive and Convective Transport in Limestone Dissolution for Wet Flue Gas Desulphurisation

Claudio Carletti^{*,a}, Cataldo De Blasio^b, Henrik Grénman^c, Tapio Westerlund^a

^aProcessDesign and Systems Engineering Laboratory, ^cLaboratory of Industrial Chemistry and Reaction Engineering, Department of Chemical Engineering, Åbo Akademi University, Biskopsgatan 8 20500, Åbo, Finland

^bLaboratory of Energy Engineering and Environmental Protection, Department of Energy Technology, Aalto University Sähkötieteiden tie 4 P.O.Box 14400, Espoo, Finland
claudio.carletti@abo.fi

Limestone dissolution has been widely studied because of its importance in different fields, a common assumption has been to consider that the roles of mass transport and chemical reaction change as a function of pH. Furthermore, a commonly accepted model for the kinetics has not been presented thus far for a wide pH range. A model which considers only diffusion based on Fick's second law and chemical reaction was derived in the present work and compared to the two-step model that takes into account both diffusion and convection with reaction. The comparison was done in terms of the Peclet (Pe) number, and the newly introduced Peclet number for the just suspended condition (Pe_j^*) which can be used to estimate the distribution of solids in the system. This approach allowed for a quantification of the differences between the assumption of only diffusion limitation and both convective and diffusive transport done in terms of the hydrodynamic factors affecting the mass transport process rather than the pH as has been widely applied in literature.

1. Introduction

Sulphur dioxide is a well-known pollutant which is harmful for human health, furthermore, it can damage infrastructure and affect ecosystems when present in the atmosphere. Limestone dissolution has been regarded as one of the rate determining steps in absorption of sulphur dioxide (SO₂) from flue gases by means of wet flue gas desulphurisation (WFGD), which is one of the leading technologies worldwide. In limestone dissolution as in any other solid-liquid reaction, both mass transport and reaction at the surface of the particles play important roles as rate determining steps. It is common to encounter industrial processes where mechanical agitation of a solid-liquid slurry operate at stirring speeds below or just above the critical suspension speed (N_{js}) at which all particles are suspended. Under such conditions, the distribution of the dispersed phase is not homogenous and significant solid concentration gradients exist (Tamburini et al., 2013). A wet flue gas desulphurisation process is likely to be controlled by mass transport rather than chemical reaction, due to the high solid loadings compared to the dissipated energy. The aim of the present study was to assess the main controlling mechanism in limestone dissolution at low pH through detailed kinetic modelling and by means of dimensionless parameters that can be used as a benchmark for process scale-up, also with the main objective of optimising the energy utilization and water consumption of the process. Limestone is dissolved with a strong acid, according to (Carletti et al., 2013),



2. First order and two-step model

The two-step model consists of a mass transfer step in the liquid phase, or transport through the diffusion layer depending on the hydrodynamics and the chemical reaction step at the solid-liquid interface (Levenspiel, 1999). If the mass transport is sufficiently enhanced, it can be assumed that the thickness of the diffusion layer is negligible and the concentrations in the solid-liquid interface or surface of the particles are equal to the bulk concentration. In a previous work (Carletti et al., 2013) a hydrodynamic regime was determined under which the dissolution rate was no longer affected by stirring speed. The chemical reaction at the surface of the particles can be expressed as

$$-V \frac{dC_{H^+}}{dt} = k_r A (C_{H^+}^j - C_{H^+}^{eq})^n \quad (2)$$

where V is the reactor volume (m^3), C_{H^+} , $C_{H^+}^j$, $C_{H^+}^{eq}$ are the hydronium ion concentrations in the bulk, at the solid-liquid interface and in equilibrium respectively (mol/L), k_r is the chemical reaction constant (m/s), A is the surface area (m^2) available for reaction and n is the order of reaction. At low values of pH ($pH \leq 4.5$) it is assumed that the effect of the equilibrium concentration is negligible as well as the effect of CO_2 on the dissolution and that n is approximately 1 and Eq(2) can be simplified.

$$r_{H^+} = k_r A C_{H^+}^j \quad (3)$$

The dissolution rate can be related to the rate of H^+ consumption, which is proportional to the interface concentration according to Eq(3), the chemical reaction step. The second step corresponds to the mass transfer between the bulk and the solid-liquid interface according to,

$$N_{H^+} = k_l (C_{H^+} - C_{H^+}^j) \quad (4)$$

where N_{H^+} is the H^+ flux ($mol/m^2 \cdot s$) and k_l is the mass transfer coefficient (m/s). The mass transfer rate is obtained after multiplying Eq(4) by the surface area of reaction (A).

$$N_{H^+} A = k_r A C_{H^+}^j \quad (5)$$

The concentration at the interface can be calculated after introducing Eq(4) in Eq(5) according to,

$$C_{H^+}^j = \frac{k_r C_{H^+}}{k_r + k_l} \quad (6)$$

Under high agitation, the mass transfer coefficient is higher than the reaction rate constant, $k_l \gg k_r$, implying that the concentration at the surface can be approximated to the bulk concentration. Thus, the dissolution is assumed to be limited by chemical reaction at the solid-liquid interface according to,

$$-V \frac{dC_{H^+}}{dt} = k_r A C_{H^+} \quad (7)$$

After integrating and providing known surface areas and reactor volumes, the reaction rate constant, k_r , can be estimated from a linear plot of $\ln(C_{H^+})$ versus time according to,

$$\ln C_{H^+} = \ln C_{H^+}^0 - \frac{k_r A}{V} t \quad (8)$$

The estimation of k_r through Eq(8) can be done only when $k_l \gg k_r$, and for very dilute suspensions under turbulent conditions with high agitation. If the mass transfer limits the reaction rate as is often in industrial applications, the mass transfer needs to be considered and estimated. The mass transfer coefficient can be estimated through the Sherwood number (Sh) for mass transfer around a spherical particle, the widely accepted equation by Ranz and Marshall can be used (Levins and Glastonbury, 1972).

$$Sh = 2 + 0.6 Re^{1/2} Sc^{1/3} \quad (9)$$

Where Re is the Reynolds number for the particle and Sc is the Schmidt number which relates the momentum to mass diffusivity. The Reynolds number can be calculated according to the Kolmogoroff's theory of local isotropic turbulence, furthermore, Re , Sc and Sh are calculated according to,

$$Re = \frac{\varepsilon^{1/3} d_p^{4/3}}{\vartheta}, \quad Sc = \frac{\vartheta}{D_{H^+}}, \quad Sh = \frac{k_l \cdot d_p}{D_{H^+}} \quad (10)$$

where D_{H^+} is the mass diffusivity of H^+ (m^2/s), ε is the average dissipated energy to the system (W/kg), d_p is the particle diameter (m) and ϑ is the kinematic viscosity (m^2/s). The mass transfer coefficient is thus calculated after introducing the dimensionless numbers from Eq(10) in Eq(9),

$$k_l = \frac{D_{H^+}}{d_p} \left(2 + 0.6 \left(\frac{\varepsilon d_p^4}{\vartheta^3} \right)^{1/6} \left(\frac{\vartheta}{D_{H^+}} \right)^{1/3} \right) \quad (11)$$

The mean dissipated energy is a function of the density, the stirring speed, the impeller diameter and a dimensionless parameter, the power number that takes into consideration the design configurations of the system.

$$\varepsilon = \frac{N_p \rho N^3 D^5}{V} \quad (12)$$

where N_p is the dimensionless power number, D is the impeller diameter (m), N is the stirring speed ($1/s$), and ρ is the density (kg/m^3). The diffusivity of the hydronium ions is a function of the temperature and is calculated according to a correlation (Boudreau, 1997),

$$D_{H^+} = \alpha + \beta \cdot T \quad (13)$$

where α and β are empirical parameters and T is the temperature ($^{\circ}C$). The mass transfer step in the two-step model considers a sum of both contributions of molecular diffusion and convection, with the limiting case of the Sherwood number approaching 2 for a spherical particle immersed in a stagnant liquid where Re approaches zero and the boundary layer thickness tends to infinity (Welty et al., 2008).

3. Diffusion model

Diffusion of hydronium ions within the boundary layer has been regarded as the rate determining step in limestone dissolution at low pH (Siagi and Mbarawa, 2009). In order to test this hypothesis, the second law of Fick in one dimension can be applied with chemical reaction by neglecting convective effects. The equation describing non-stationary transport with diffusion and chemical reaction becomes,

$$\frac{\partial C_{H^+}}{\partial t} = D_{H^+} \frac{\partial^2 C_{H^+}}{\partial x^2} - k_r C_{H^+} \quad (14)$$

The equation above needs two boundary conditions to be solved, the origin of the system is set at the limit of the boundary layer, thus $x=0$ and Eq(14) is solved in order to obtain the concentration as a function of time (t) and the coordinate x , the boundary conditions are,

$$\begin{aligned} x=0, t>0, C_{H^+} &= C_{H^+}^o \\ x \rightarrow \infty, t>0, C_{H^+} &= 0 \end{aligned} \quad (15)$$

At $x=0$ the concentration of H^+ corresponds to the concentration at the boundary layer, or at the bulk, while at a position further away from the origin, the H^+ concentration tends to zero. The second law of Fick with chemical reaction, Eq(14), can be solved after introducing a change of variable and applying the Laplace transformation to obtain an ordinary differential equation which can be solved with a general solution, finally the solution is anti-transformed from the Laplace domain into the x and t domain giving,

$$C_{H^+} = \frac{C_{H^+}^o}{2} \left[e^{-\sqrt{\frac{k_r}{D_{H^+}}} x} \operatorname{erfc} \left(\frac{x}{2\sqrt{D_{H^+} t}} - \sqrt{k_r t} \right) + e^{\sqrt{\frac{k_r}{D_{H^+}}} x} \operatorname{erfc} \left(\frac{x}{2\sqrt{D_{H^+} t}} + \sqrt{k_r t} \right) \right] \quad (16)$$

In order to compare the diffusion model and the two-step model, it is necessary to determine the distance at which the solid-liquid interface is positioned, this distance is known as the thickness of the boundary layer δ (m). The application of the first law of Fick for spherical particles in steady state gives,

$$N_i A = -4\pi r^2 D_i \frac{dC}{dr} \quad (17)$$

where r is the radius and D_i is the diffusivity (m^2/s) of species i . After integrating Eq(17) from the radius of the particle (R), until $(R+\delta)$ the following expression is obtained,

$$N_i \cdot A = 4\pi D_i \frac{(C-C')}{\left(\frac{1}{R+\delta} - \frac{1}{R}\right)} \quad (18)$$

The expression in Eq(18) can be substituted into an expression of the form of Eq(4) in order to find δ . After substituting the radius with $d_p/2$ and the Sherwood number defined in Eq(10), the following expression is obtained for the boundary layer thickness,

$$\delta = \frac{d_p}{2 - Sh} \quad (19)$$

4. Convective and diffusive transport

As it was mentioned above, diffusive transport has been regarded as the main controlling mechanism in limestone dissolution and the effect of convective transport has thus been neglected. Nonetheless, this assumption can be quantitatively assessed through the Peclet number which is defined as the ratio between convective to diffusive transport.

$$Pe = Re \cdot Sc = \frac{v \cdot L}{D_i} \quad (20)$$

When the convective transport dominates, the Peclet number is large and diffusion through the boundary layer may be the determining step, this occurs specially under high agitation when all solids are suspended and possibly equally distributed in the reactor vessel. In industry this is seldom the case as the process is operated around N_{js} and the solid distribution which is certainly not uniform affects the process performance (Tamburini et al., 2013). The newly introduced Peclet number at the just suspended speed (Pe^*) can be used to assess the solid distribution by means of a dimensionless number (Carletti et al., 2014).

$$Pe^* = \frac{U_t H_L}{D_{es}} \quad (21)$$

where U_t is the particle settling velocity (m/s) and D_{es} corresponds to the relative axial solid dispersion coefficient and it is calculated according to,

$$D_{es} = a(N - N_{js})D^2 \quad (22)$$

Where a is a dimensionless parameter, equal to 0.12 for a 4 blade PBT impeller. The settling velocity is calculated after applying a balance of forces to the particle having a settling velocity, and the N_{js} is obtained by means of the well-known Zwietering correlation (Carletti et al., 2014).

5. Materials and methods

The experimental set-up consisted of a 2 L glass reactor with 4 equally spaced stainless steel baffles, a mixed flow impeller pumping downwards with 4 pitched blades having a 45° inclination (PBT), a pH electrode, a pH meter (EDT Micro 2) having automatic temperature compensation and a device for temperature control (Thermomix 1441 B. Braun). The pH meter was calibrated before each experiment with a four point calibration procedure using pH buffers of 2.00, 5.00, 7.00 and 10.00 at room temperature (23 °C). The temperature was measured by means of a thermocouple; the values of pH and temperature were recorded by using a data acquisition system (Personal Daq/55). All experiments were performed letting pH drift under transient conditions, i.e. the free drift method, where 1 g of solid sample is added into 1.5 L of de-ionized water and 60 mL of HCl, the reaction took place from pH 2.4 until 5. The samples employed were from Wolica, Poland and Parainen Finland having different geological provenience. The Wolica sample is sedimentary, from the Jurassic age and the Parainen a metamorphic sample from the Proterozoic age. Both samples are composed mainly of the mineral calcite having a composition higher than 98 % CaCO₃. The samples were crushed and fractionated with a 212-215 μm sieve, particle size distribution (PSD) of the samples was performed before and after reaction by means of laser diffraction (Malvern Mastersizer 3000). Furthermore, Scanning Electron Microscopy (SEM) was also employed to study the shape and morphology of the samples, specific surface area values (SSA) that were previously measured were used (Carletti et al., 2013). The experiments were performed at 7 different stirring speeds for every sample, the highest two stirring speeds were used to calculate the chemical reaction constant, while the rest were employed to compare the diffusion model with

the two-step model. All experiments were performed with temperature control at 20 ± 1 °C. The experimental set-up and a SEM image of a reacted sample are shown in Figure 1.

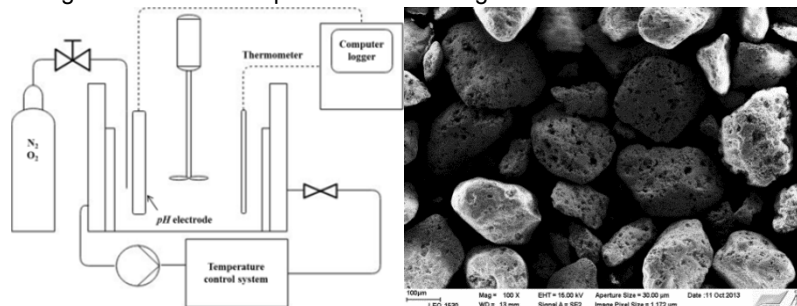


Figure 1: Experimental set-up (left) and Wolica sample after reaction (right).

6. Results and discussions

The PSD results were fitted to a Log-Normal distribution and two cases are shown in Figure 2 along with the change in C_{H^+} concentration as a function of time for the Parainen sample at different stirring speeds.

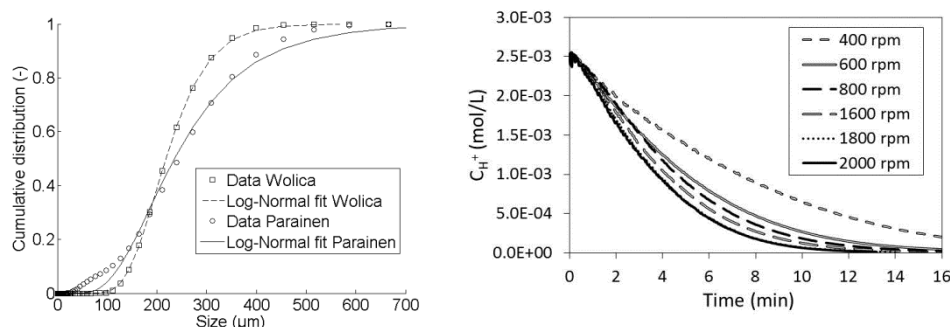


Figure 2: PSD of the Parainen sample before reaction, Wolica sample after reaction (left) and effect of stirring for the Parainen sample (right).

Figure 2 shows that above 1800 rpm, $N=3 \cdot N_{js}$, the stirring doesn't seem to affect the dissolution. It is assumed that, at the stirring speeds of 1800 and 2000 rpm, the dissolution rate can be modelled according to Eq(7) which gives a linear function of the C_{H^+} where the slope is a function of k_r , the volume (V) and the surface of reaction (A), estimated between PSD and SSA. Therefore, the chemical rate constant, k_r , can be estimated after plotting $\ln(C_{H^+})$ versus time, shown in Figure 3, for the cases where $k_r \ll kl$. Furthermore, the mass transfer coefficient is calculated by using Eq(11).

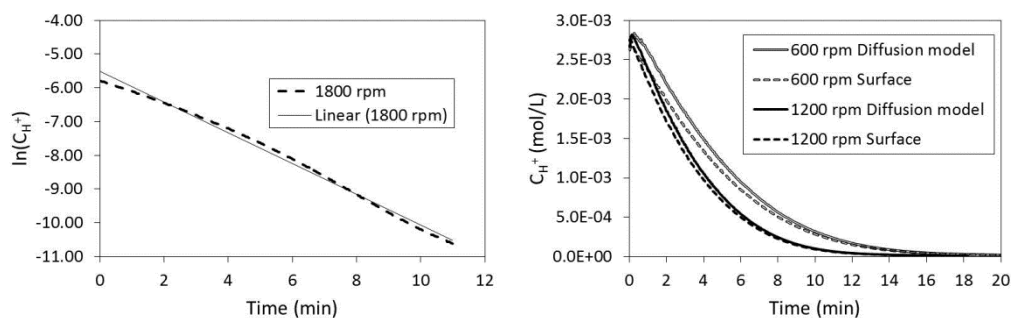


Figure 3: First order plot in the kinetic regime for Wolica sample (left) and the two-step model (surface) compared to the diffusion model for Wolica sample in the mass transfer limited regime (right).

The comparison between the diffusion model with chemical reaction and the two-step model can be done by using Eq(16) to calculate $C_{H^+}^i$ at the distance of $x=\delta$, which is calculated from Eq(19), and by calculating the

$C_{H^+}^j$ according to the two-step model from Eq(6). The comparison of the two models with Pe and $1/Pe^*$ is shown in Figure 4, the results show that the two models are closer at higher stirring speeds (Figure 4 left). The model considering both phenomena and the one considering only diffusion tend to approach at higher values of Pe due to diffusion control within the boundary layer over convective transport in the bulk. However, the models deviate when convective transport starts to be rate limiting, i.e. at lower values of Pe .

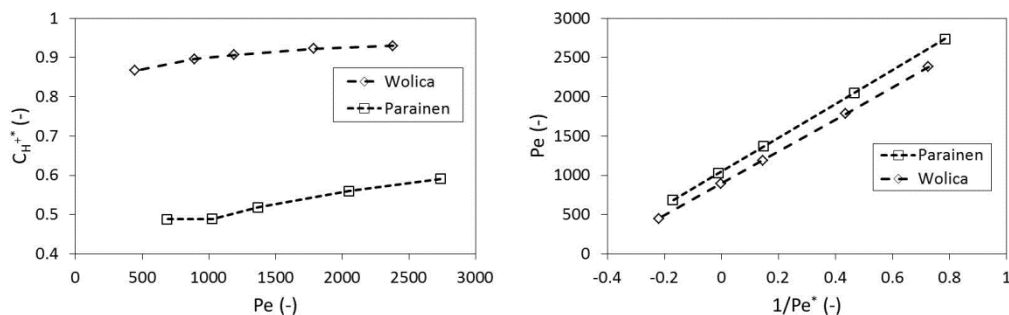


Figure 4: Dimensionless concentration as a function of Peclet (left) and Peclet number versus the inverse of the Peclet number at the critical stirring speed $1/Pe^*$.

The assessment of the effect of diffusion and convection is done by plotting the dimensionless concentration, $C_{H^+}^*$, which is calculated by dividing interface concentration obtained from the two-step model, Eq(6), with the interface concentration obtained from the diffusion model versus Pe , Eq(16). Figure 4 shows a clear correlation between $C_{H^+}^*$, the Peclet number and between the two Peclet numbers.

7. Conclusions

Limestone dissolution was investigated by mean of experimental analysis and detailed modelling. A two-step model was compared with a diffusion model with reaction by means of the Peclet number in order to properly assess the controlling mechanisms of limestone dissolution. This approach shows that, when operating around N_{js} for the Wolica sample ($1/Pe^*$ equal to zero) convection may contribute only 10 %, however, for the Parainen sample at the N_{js} , convection may contribute as much as 50 %. Furthermore, this method also allows the estimation of how well the solids are dispersed, by means of the Pe^* , which is directly correlated to the degree of mixing and could serve as a benchmark for process scale-up.

Acknowledgements

The authors wish to express their gratitude to the Graduate School in Chemical Engineering (GSCE).

References

- Boudreau B. P., 1997. Diagenetic Models and their implementation, modelling transport and reactions in aquatic sediments, Heidelberg: Springer.
- Carletti C., Grénman H., De Blasio C., Westerlund T., 2013. Limestone dissolution study for wet flue gas desulfurization under turbulent regimes above critical suspension speed, Computer-Aided Chemical Engineering, 32, 301-306.
- Carletti C., Montante G., Westerlund T., Paglianti A., 2014. Analysis of solid concentration distribution in dense solid-liquid stirred tanks by electrical resistance tomography, Chemical Eng Science, 119, 53-64.
- Levenspiel O., 1999, Chemical reaction engineering. John Wiley and Sons Inc, USA.
- Levins D. M., Glastonbury, J. R., 1972, Application of Kolmogoroff's theory to particle-liquid mass transfer in agitated vessels, Chemical Engineering Science, 27, 537-543.
- Siagi Z. O., Mbarawa M., 2009, Dissolution rate of South African calcium based materials at constant pH. Journal of Hazardous Materials, 163, 678-682.
- Tamburini A., Cipollina A., Micale G., Brucato A., Ciofalo M., 2013. CFD Prediction of Solid Particle Distribution in Baffled Stirred Vessels under Partial to Complete Suspension Conditions, Chemical Engineering Transactions, 32, 1447-1452.
- Welty J. R., Wicks C. E., Wilson R. E., Rorrer G. L., 2008, Fundamentals of momentum, heat and mass transfer. 5th ed., John Wiley & Sons Inc., Ney York, USA.